Journal of Alloys and Compounds 526 (2012) 68–73

Contents lists available at SciVerse ScienceDirect

Journal of Alloys and Compounds

journal homepage: www.elsevier.com/locate/jallcom

Effect of Co on the microstructure, magnetic properties and thermal stability of bulk $Fe_{73-x}Co_xNb_5Y_3B_{19}$ (where $x = 0$ or 10) amorphous alloys

Marcin G. Nabialek[a,*], Michal Szota[b], Marcin J. Dospial[a]

[a] Institute of Physics, Czestochowa University of Technology, 19 Armii Krajowej Av., 42-200 Czestochowa, Poland
[b] Institute of Materials Engineering, Czestochowa University of Technology, 19 Armii Krajowej Av., 42-200 Czestochowa, Poland

ARTICLE INFO

Article history:
Received 9 July 2011
Received in revised form 16 February 2012
Accepted 17 February 2012
Available online xxx

Keywords:
Amorphous materials
Ferromagnetic materials
Magnetic hysteresis
X-ray measurements
DSC curves
Point and linear structural defects

ABSTRACT

The paper presents the results of structure, thermal stability and magnetic properties of bulk $Fe_{73-x}Co_xNb_5Y_3B_{19}$ (where $x = 0$ or 10) amorphous alloys in the as-cast state, in the form of 0.5 mm thick plates with an area of 100 mm^2. The amorphous structure of the investigated alloys was confirmed by studies of Mössbauer effect and X-ray diffractometry. On the basis of measurements performed using a vibrating sample magnetometer (VSM), it was found that substituting 10% of Fe with Co in $Fe_{73-x}Co_xNb_5Y_3B_{19}$ alloy, had only a small effect on the value of saturation magnetization ($\mu_0 M_S$), and was of the same importance in terms of the values of the coercivity field (H_C) and the Curie temperature (T_C).

The magnetization for both samples increases in high magnetic fields due to rotation of magnetic moments near the structural defects called quasidislocalised dipoles, near the area known as the approach to ferromagnetic saturation. For field values with a linear relationship $(\mu_0 H)^{-1}$ of the reduced saturation magnetization (M/M_S), further increase of the magnetization for the studied samples is associated with the Holstein–Primakoff process, which is under the influence of dumping of thermally activated spin-waves.

The curves of thermal analysis, obtained using differential scanning calorimetry (DSC), show that Co reduces the glass transition and primary crystallization temperatures.

The results of this study indicate that substituting 10% of Fe with Co in ferromagnetic $Fe_{73}Nb_5Y_3B_{19}$ alloy causes the deterioration of its so-called soft magnetic properties and decreases the Curie temperature and the primary crystallization temperature.

1. 1 Introduction

Amorphous alloys, based on Fe, are extremely interesting due to their magnetic as well as mechanical properties [1,2]. These alloys have the potential to replace currently used amorphous or nanocrystalline laminated ribbons, used in modern transformer cores. It is well known that amorphous ribbons are produced at high cooling speeds, which has a significant influence on their thickness, typically ranging over tens of microns. The possibility of using thin ribbons as electrotechnical materials is limited, therefore, there have been attempts to obtain ready-made amorphous magnetic cores of various geometric shapes and large thicknesses. Some of the first bulk amorphous magnetic materials based on Fe were prepared in 1995. Since then, a number of bulk amorphous alloys, based on Fe, Co or Ni, characterized by good soft magnetic and mechanical properties, were created [3–8]. The following qualities make these materials extremely attractive for application:high saturation magnetization, negligible value of coercivity field and low core losses, in combination with high microhardness as well as wear and corrosion resistance [8–10].

Searches are being conducted to discover new, inexpensive, simple in terms of chemical composition, amorphous alloys, in which the main component is magnetic Fe. Modelling of soft magnetic properties of Fe alloys can be achieved through making changes in the quantity of magnetic elements, such as Co or Ni, in its composition [11].

The paper presents the results of the structural, magnetic properties and thermal stability examinations of bulk $Fe_{73-x}Co_xNb_5Y_3B_{19}$ ($x = 0$ or 10) amorphous alloys, manufactured in the form of 0.5 mm thick plates, using the suction-casting method.

2. Experimental procedures

Samples of $Fe_{73-x}Co_xNb_5Y_3B_{19}$ ($x = 0$ or 10) alloys were produced in the form of 0.5 mm thick plates, each with an area of approximately 100 mm^2. The components used for the preparation of crystalline ingots had purities of: Fe – 99.98%, Y – 99.98% Nb – 99.999% and Co – 99.98%. Boron was added as $Fe_{54.6}B_{45.4}$ alloy. Samples were

* Corresponding author. Fax: +48 34 3250795.
E-mail address: nmarcell@wp.pl (M.G. Nabialek).

0925-8388/$ – see front matter © 2012 Published by Elsevier B.V.
doi:10.1016/j.jallcom.2012.02.106

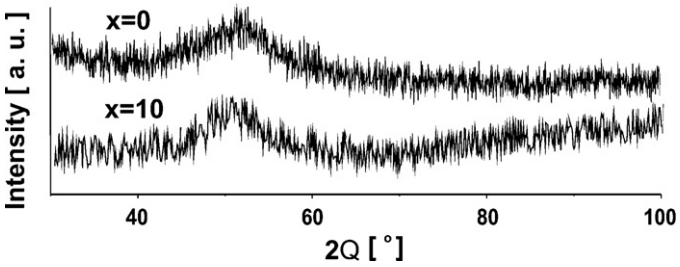

Fig. 1. X-ray diffraction pattern (CoK_α) obtained for the $Fe_{73-x}Co_xNb_5Y_3B_{19}$ alloys.

obtained using a device, which performed the suction of liquid alloy into a cooled, copper mould.

The microstructure of alloys in the as-cast state was studied using: X-ray diffraction (CoK_α), Mössbauer Spectroscopy (^{57}Fe) and scanning electron microscopy. Static hysteresis loops were measured at room temperature using a "LakeShore" vibrating sample magnetometer. The Curie temperature was determined from measurements made in a constant magnetic field with intensity of 0.7 T, using Faraday magnetic weight measuring equipment.

On the basis of Kronmüller's work [12] the influence of structural defects on the magnetization process was studied, in the area known as approach to ferromagnetic saturation. DSC curves were obtained from the measurements made using the "Netzsch" differential scanning calorimeter.

3. 3 Results and discussion

X-ray diffraction patterns obtained for samples of all investigated alloys are shown in Fig. 1.

Both diffraction patterns look similar. It is not possible to distinguish the presence of narrow peaks evidencing the occurrence of periodic crystalline structure; on the contrary there are visible broad maxima, typical for amorphous materials. The amorphous structure of investigated samples was also confirmed by ^{57}Fe Mössbauer Spectroscopy studies as shown in Fig. 2.

The Mössbauer spectra, depicted in Fig. 2, consist of broad, asymmetric, overlapping lines. These spectra are typical for materials with an amorphous structure. The distributions of hyperfine field induction, obtained from the analysis of these spectra, are asymmetric and it is possible to distinguish at least two components therein, indicating the presence of areas of both high and low iron content, created during the solidification process.

The average value of hyperfine field induction for both investigated alloys is higher than 14 T; this confirms that in the manufactured alloys, the vast majority of resonant Fe atoms are in the ferromagnetic state.

Fig. 3 shows the scanning electron microscope pictures of structures, for the fractures of investigated samples in the as-cast state.

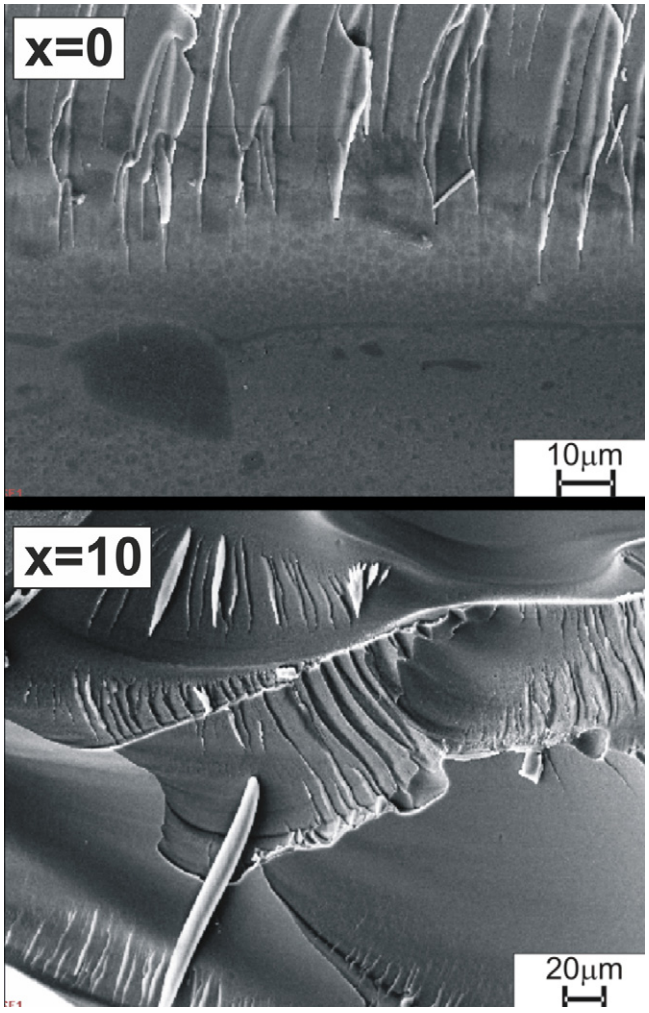

Fig. 3. SEM pictures of structures for the fractures of produced alloys.

Fractographical studies have shown that the obtained fractures are typical of a relaxed amorphous structure. Smooth fractures are predominant for the obtained images of fractures of the investigated plates. The morphology of the fractures, corresponding to the sample of $Fe_{73}Nb_5Y_3B_{19}$ alloy (except for the smooth fracture) shows poorly developed band scales and surface irregularities.

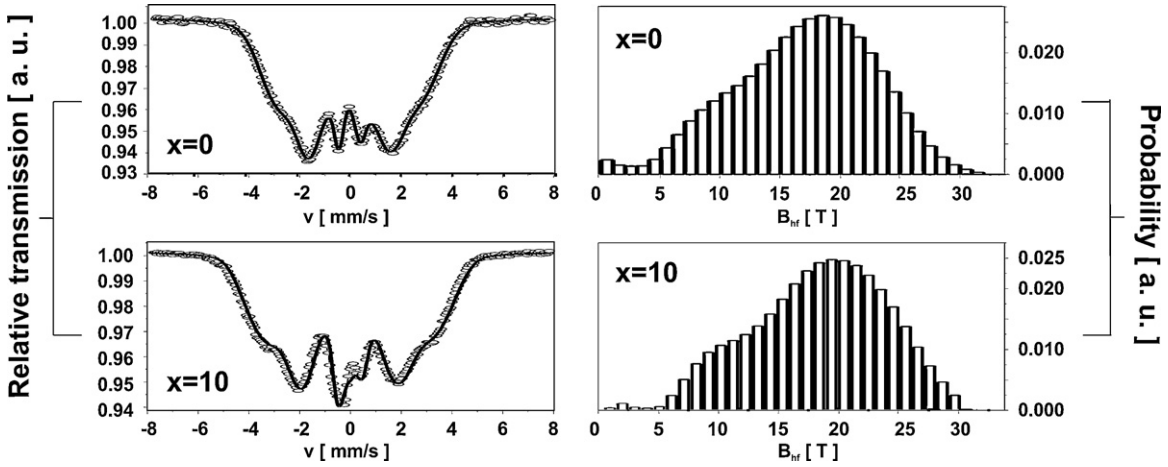

Fig. 2. Transmission Mössbauer spectra and corresponding hyperfine field distributions of the induction, obtained for samples in the as-cast state.

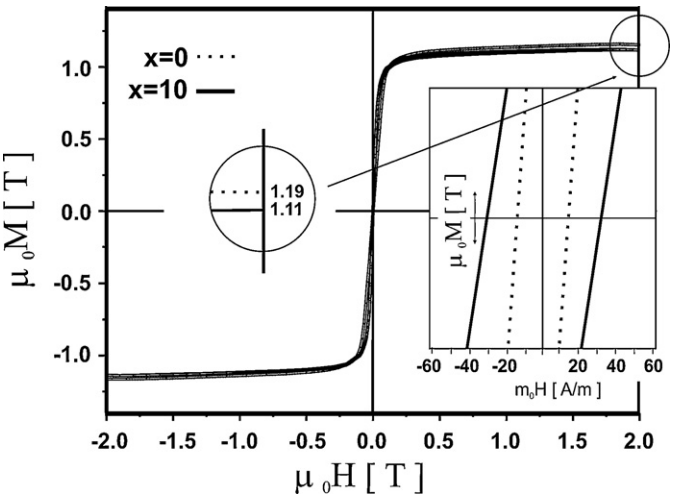

Fig. 4. Static hysteresis loops measured for $Fe_{73-x}Co_xNb_5Y_3B_{19}$ alloys in the as-cast state.

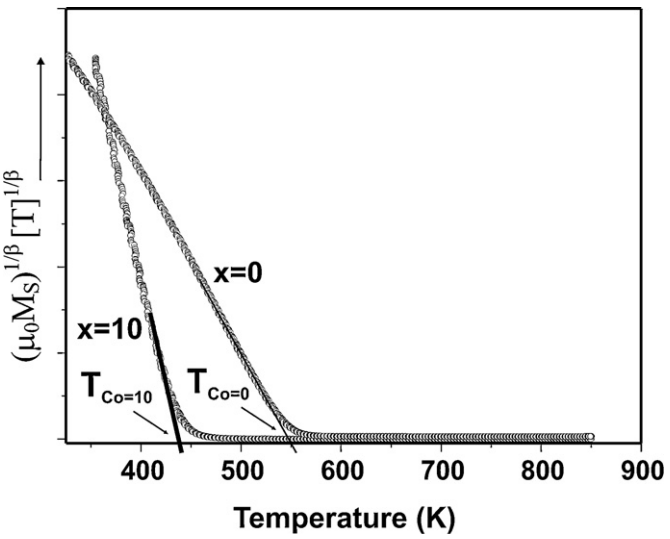

Fig. 5. $(\mu_0 M_S)^{1/\beta}$ temperature dependence measured for alloys in the as-cast state.

Fig. 3 (for $x = 10$) shows a quite interesting cascade area of the fracture with visible levels, where alternately smooth or scaly fractures can be observed.

The saturation of both magnetization and coercive field are very important parameters for the use of magnetically soft ferromagnetic materials. The static hysteresis loops measured for manufactured samples of $Fe_{73-x}Co_xNb_5Y_3B_{19}$ ($x = 0$ or 10) alloys in the form of plates are shown in Fig. 4.

It can be concluded from the shape of the static hysteresis loops that both investigated alloys have a similar value of saturation magnetization. However, as observed in Fig. 4, 10% addition of atomic Co at the expense of Fe in the bulk $Fe_{73}Nb_5Y_3B_{19}$ alloy results in a slight reduction in the value of saturation of the magnetization. Moreover, according to the obtained experimental data, the previously described addition of Co causes a significant reduction in the coercivity field, which for the studied samples of $Fe_{63}Co_{10}Nb_5Y_3B_{19}$ and $Fe_{73}Nb_5Y_3B_{19}$ alloys, equals 16 A/m and 32 A/m, respectively. These results are consistent with the results, presented in work related to bulk amorphous alloys by other authors [10,13–15]. Tiberto et al. [15], in addition to results of studies related to bulk amorphous materials, included results for amorphous materials in the form of thin ribbons, which show that the gradual replacement of Fe with Co increases the saturation magnetization and the coercivity field. In the investigated bulk plates, the value of coercivity field is quite high, which can be explained by the presence of structural defects, created during the solidification process. The presence of such defects, which may take the form of domain walls pinning sites, causes an increase in the coercivity field. Areas at which structural defects are formed possess beneficial energy conditions to become the nucleation centres for the crystalline phase.

The Curie temperature of a ferromagnetic alloy is an important parameter defining its extent of applicability (Fig. 5).

The polarity of the magnetic saturation $\mu_0 M_S$, as a function of temperature T at constant magnetic field strength of 0.6 T, was measured using Faraday's magnetic weight. The Curie temperature (T_C) for all investigated alloys in the form of plates in the as-cast state was identified; the following dependence was used: $(\mu_0 M_S)^{1/\beta}$ (where β is the critical exponent equal to 0.36), in the $\mu_0 M_S = \mu_0 M_0 (1 - T/T_c)^{\beta}$ equation ($\mu_0 M_0$ – magnetic saturation of the polarization at $T = 0$ K) for the ferromagnet meeting Heisenberg assumptions [16].

The results indicate that the addition of Co, at the expense of Fe, radically effects a reduction of the Curie temperature. In the presented temperature range, a single transition from ferromagnetic to paramagnetic state was observed. In references [17,18] it was shown that in amorphous materials, the preferred crystalline phase $(Fe, Co)_{23}B_6$ is present, with the Curie temperature of 698 K [19,20]. In the studied alloys, at the specified temperature, magnetic transition was not observed. As the distributions of hyperfine field induction obtained from transmission Mössbauer spectra indicate, in the volume of investigated samples there are no areas that could be attributed to the presence of $(Fe, Co)_{23}B_6$ phase, which would be reflected by clearly separated field components [19].

The lack of translational symmetry and angular correlations in the arrangement of atoms in amorphous alloy prevents the formation of structural defects as normally expected to occur in conventional crystalline materials. Any deviation from the system of atoms in the liquid state which find themselves in the thermodynamic equilibrium is considered to be a structural defect in amorphous alloys [21]. One common type of defect, characteristic of the amorphous state, is a so-called 'free volume' (Fig. 6), which plays a similar role to that of a point defect in the crystalline material [22].

The structural relaxation, occurring during the production of amorphous alloys or during the heat treatment, causes the migration of free volumes to the sample surface, their annihilation and creation of three-dimensional agglomerations. Large three-dimensional agglomerations of free volumes are not stable and after their disintegration they form flat defects, called quasidislocalised dipoles. The defects present in amorphous alloys are sources of internal stresses, which affect the magnetization process. A

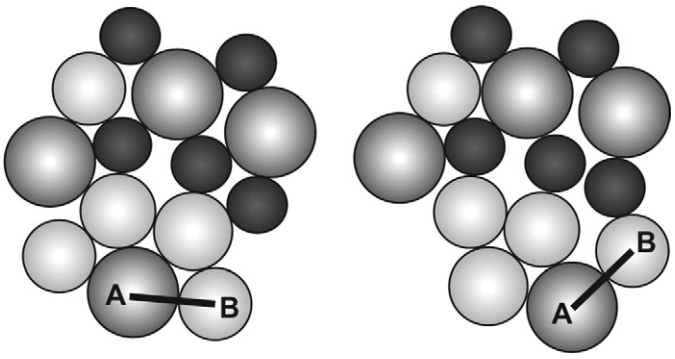

Fig. 6. Schematic of free volumes in the amorphous material [22].

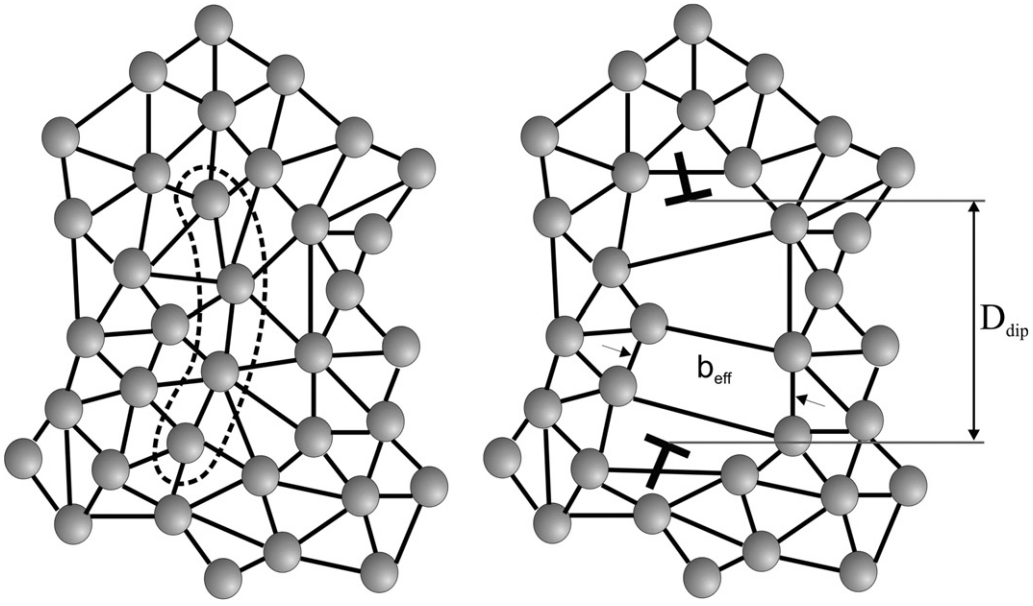

Fig. 7. Model of quasidislocalised dipole: b_{eff}–length of effective Burgers' vector, D_{dip} – width of the quasidislocalised dipole [22].

two-dimensional schematic diagram of quasidislocalised dipoles in amorphous alloy is presented in Fig. 7 [23].

The type and influence of structural defects on the magnetization process in amorphous alloys was examined using the H. Kronmuller theory [12,24]. The magnetization, in strong magnetic fields near the area known as the approach to ferromagnetic saturation, can be described by the relation:

$$M(H) = M_S\left[1 - \frac{a_{1/2}}{(\mu_0 H)^{1/2}} - \frac{a_1}{(\mu_0 H)^1} - \frac{a_2}{(\mu_0 H)^2}\right] + b(\mu_0 H)^{1/2}, \quad (1)$$

expression $\frac{a_{1/2}}{(\mu_0 H)^{1/2}}$ appearing in Eq. (1) is associated with the presence of point defects in the volume of the amorphous sample, while the expressions $\frac{a_1}{(\mu_0 H)^1}$ and $\frac{a_2}{(\mu_0 H)^2}$ are assigned to the presence of defects called quasidislocalised dipoles. At higher magnetic fields where the dependencies $\left[\frac{a_{1/2}}{(\mu_0 H)^{1/2}}, \frac{a_1}{(\mu_0 H)^1}, \frac{a_2}{(\mu_0 H)^2}\right]$ are not met, the rotation of the magnetization vector is caused by the suppression of thermally excited spin waves, and this phenomenon is called the Holstein–Primakoff process, which is expressed by the formula (2) [25].

$$\Delta M_{sp} = b(\mu_0 H)^{1/2}, \quad (2)$$

where b is the coefficient specified on the basis of the spin waves theory [26].

The analysis of the reduced magnetization curves M/M_S in high magnetic fields reveals linear functions of $(\mu_0 H)^{-1}$, for the magnetic fields in the range from 0.68 T to 0.12 T for the sample of $Fe_{73}Nb_5Y_3B_{19}$ alloy (Fig. 8 for $x = 0$) and from 0.69 T to 0.05 T for the sample of $Fe_{63}Co_{10}Nb_5Y_3B_{19}$ alloy (Fig. 8 for $x = 10$).

Observed changes in the magnetization (Fig. 8) indicate that the magnetization process, in a specified range of magnetic fields, is related to the rotation of magnetic moments within the structural defects (quasidislocalised dipoles), where the dependence $D_{dip} l_H^{-1} < 1$ is met (D_{dip} width of quasidislocalised dipole, and l_H^{-1} exchange length). For higher values of the magnetic fields, above 0.7 T, considering all of the investigated alloys, the Holstein–Primakoff process was observed (Fig. 9) [25]. Parameters obtained from the analysis of the reduced saturation of magnetization curves, as functions of $(\mu_0 H)^{-1}$ and $(\mu_0 H)^{1/2}$, are shown in Table 1.

The data collected in Table 1 indicate that the real density of structural defects present in the samples, is slightly smaller for the sample with the Co addition. A slight increase in the size of structural defects, present in the $Fe_{63}Co_{10}Nb_5Y_3B_{19}$ alloy, is directly related to the atomic composition of the alloy. It is important that during the preparation of all investigated samples the same manufacturing conditions were preserved i.e., chamber atmosphere, under which the liquid alloy was sucked into the copper mould, the temperature of mould and the suction pressure. It should be noted that the addition of 10% of the atomic Co to the $Fe_{63}Co_{10}Nb_5Y_3B_{19}$ alloy leads to changes in the short-range ordering between atoms, which certainly have an influence on the microstructure and the stability of the amorphous state, as well as magnetic and mechanical properties. In addition, the structural defects created during the manufacturing process are defined as redundant volume; as mentioned earlier, they are the source of internal mechanical

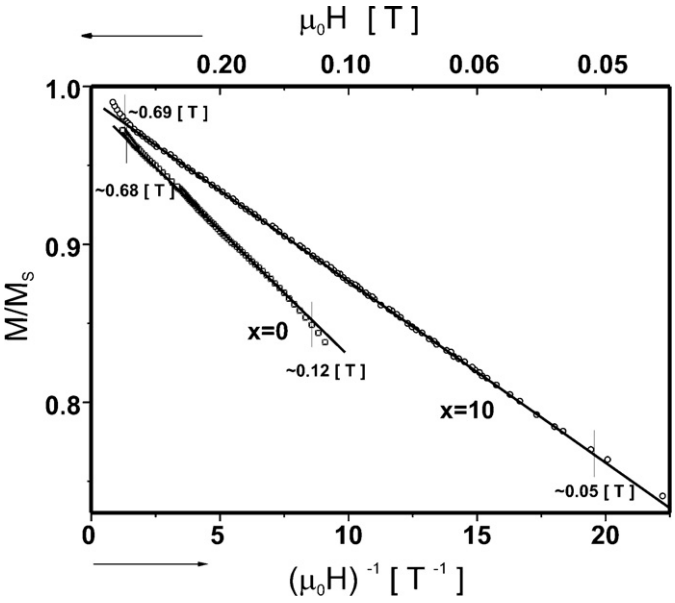

Fig. 8. The dependence of M/M_S as a function of $(\mu_0 H)^{-1}$ obtained for $Fe_{73-x}Co_xNb_5Y_3B_{19}$ alloys in the as-cast state.

Table 1
Data obtained from the analysis of the relative magnetization as a function of magnetic field strength in powers of: −1 and ½. The parameters a_1 and b are the fit parameters of the relative magnetization as functions of $(\mu_0 H)^{-1}$, $(\mu_0 H)^{1/2}$, respectively; D_{sp} – the stiffness of spin wave parameter, A_{ex} – exchange constant, D_{dip} – the width of quasidislocalised dipoles and N – the surface density of quasidislocalised dipoles.

Alloy composition	a_1 (10^{-2} T)	b (10^{-2} T$^{1/2}$)	A_{ex} (10^{-12} Jm^{-1})	D_{sp} (10^{-2} meVnm^2)	D_{dip} (nm)	N (10^{16} m^{-2})
$Fe_{73}Nb_5Y_3B_{19}$	0.0164	0.0650	1.602	41.128	2.231	20.098
$Fe_{63}Co_{10}Nb_5Y_3B_{19}$	0.0116	0.0484	1.819	50.063	2.443	16.754

Table 2
Parameters obtained from DSC curves: T_g – glass transition temperature (onset temperature on the endothermic event), T_x – onset crystallization temperature, $\Delta T_x = T_x - T_g$ – extent of the supercooled liquid region, $\Delta T_l = T_l - T_x$ undercooled temperature, $T_{rg} = T_g/T_l$ reduced glass transition temperature, T_m – onset melting temperature, T_l – onset liquid temperature, ΔT_m – interval temperature determined from the onset to the end temperature of melting process $T_l - T_m$, γ_m – modified GFA parameter which was defined as $(2T_x - T_g)/T_l$.

Alloy composition	T_g [K]	T_x [K]	ΔT_x [K]	ΔT_l [K]	T_{rg} [K]	T_m [K]	T_l [K]	ΔT_m [K]	γ_m	Sample thickness [mm]
$Fe_{63}Co_{10}Y_3B_{19}Nb_5$	858	899.5	41.5	605,5	0.57	1349	1505	156	0.63	0.5
$Fe_{73}Y_3B_{19}Nb_5$	902	947	45	501	0.62	1397	1448	51	0.68	0.5

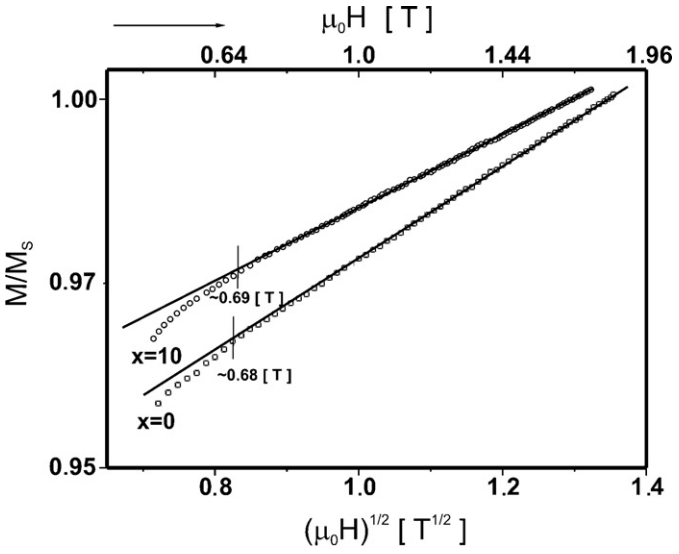

Fig. 9. The dependence of M/M_S as a function of $(\mu_0 H)^{1/2}$ obtained for $Fe_{73-x}Co_xNb_5Y_3B_{19}$ alloys in the as-cast state.

stresses, which in terms of magnetic properties is reflected by an inhomogeneous distribution of magnetic moments, induced by magneto-elastic interactions and a different exchange distance for the ferromagnetic interaction between magnetic Fe and Co atoms.

The stability of the amorphous state for the investigated alloys was determined from the analysis of DSC curves (Fig. 10).

The study of heat flow, as a function of temperature, was performed at a heating rate of 10 K/min within a temperature range from 500 K to 1600 K and its results are presented in Fig. 10. In order to achieve greater transparency of the presented results, the plot range has been reduced to the temperature of 1200 K. Both DSC curves (Fig. 10) clearly demonstrate the single, exothermic maximum, describing the crystallization of the investigated alloys. The 10% substitution of atomic Fe with Co in the alloy composition,

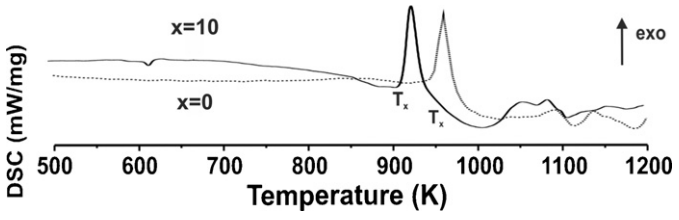

Fig. 10. Selected region of the DSC curves, measured for samples of $Fe_{73-x}Co_xNb_5Y_3B_{19}$ alloys.

causes a significant decrease in the onset of crystallization process temperature and reduces GFA (Glass Forming Ability). The parameters determined from the analysis of the DSC curves are shown in Table 2.

4. Conclusions

The obtained $Fe_{73-x}Co_xNb_5Y_3B_{19}$ ($x = 0$ or 10) alloys in the as-cast state, in the form of 0.5 mm thick plates, were fully amorphous.

The 10% substitution of atomic Fe with Co resulted in a slight decrease in the GFA, as well as a contribution to the reductions of the saturation of the magnetization, the Curie temperature, the glass transition temperature and the crystallization temperature.

The magnetization process in strong fields, near the so-called area of approach to ferromagnetic saturation, for both alloys is related to the rotation of the magnetization vector within the structural defects, called quasidislocalised dipoles. With $D_{dip} l_H^{-1} < 1$ dependence met, the Holstein–Primakoff process begins at comparable values of magnetic field strength for both alloys. A radical reduction in the coercivity was observed after the addition of Co.

In conclusion, despite the negative effect of substituting Fe with Co, which results in the decrease of the saturation of magnetization, Curie temperature and thermal stability, it is clear that such a slight deterioration of these parameters is compensated with a significant reduction of the coercivity field values. Although the Curie temperature, after the 10% addition of atomic Co at the expense of Fe, decreased by more than 100 K, it still far exceeds the operating temperature of components installed in commercially produced electrical equipment. Amorphous alloys with the addition of Co, simple in terms of chemical composition, can be successfully used as magnetic cores in modern medium power transformers.

Acknowledgments

This work was supported by the Ministry of Science and Higher Education of Poland through grant no. N N508 586639

References

[1] Y. Fu, T. Miyao, J.W. Cao, Z. Yang, M. Masumoto, X.X. Liu, A. Morisako, J. Magn. Magn. Mater. 308 (2007) 165–169.
[2] X.J. Gu, S. Joseph Poon, Gary J. Shiflet, Michael Widom, Acta Mater. 56 (2008) 88–94.
[3] S.F. Guo, L. Liu, X. Lin, J. Alloys Compd. 478 (2009) 226–228.
[4] A. Inoue, Acta Mater. 48 (2000) 279–306.
[5] D.H. Hu, G. Duan, W.L. Johnson, C. Garland, Acta Mater. 52 (2004) 3493–3497.
[6] M. Nabialek, M. Dospial, M. Szota, P. Pietrusiewicz, J. Jedryka, J. Alloys Compd. 509 (2011) 3382–3386.
[7] Q.J. Chen, H.B. Fan, J. Shen, J.F. Sun, Z.P. Lu, J. Alloys Compd. 407 (2006) 125–128.
[8] M. Nabialek, M. Dospial, M. Szota, J. Olszewski, S. Walters, J. Alloys Compd. 509S (2011) S155–S160.

[9] M.G. Nabialek, M.J. Dospial, M. Szota, Phys. Status Solidi C 7 (5) (2010) 1428–1431.
[10] S.F. Guo, Z.Y. Wu, L. Liu, J. Alloys Compd. 468 (2009) 54–57.
[11] A. Inoue, B. Shen, A. Takeuchi, Mater. Sci. Eng. A 441 (2006) 18–25.
[12] H. Kronmüller, IEEE Trans. Magn. MAG-15 (1979) 1218–1225.
[13] M.G. Nabialek, M. Szota, M.J. Dospial, P. Pietrusiewicz, S. Walters, J. Magn. Magn. Mater. 322 (2010) 3377–3380.
[14] D.S. Song, J.-H. Kim, E. Fleury, W.T. Kim, D.H. Kim, J. Alloys Compd. 389 (2005) 159–164.
[15] P. Tiberto, R. Piccin, N. Lupu, H. Chiriac, M. Baricco, J. Alloys Compd. 483 (2009) 608–612.
[16] R. Reissem, M. Seeger, H. Kronmüller, J. Magn. Magn. Mater. 128 (1993) 321–340.
[17] A. Hirata, Y. Hirotsu, K. Amiya, N. Nishiyama, A. Inoue, Phys. Rev. B 80 (2009) 140201.
[18] J. Fornell, S. Gonzalez, E. Rossinyol, S. Surinach, M.D. Baro, D.V. Louzguine-Luzgin, J.H. Perepezko, J. Sort, A. Inoue, Acta Mater. 58 (2010) 6256–6266.
[19] S. Lesz, R. Babilas, M. Nabiałek, M. Szota, M. Dośpiał, R. Nowosielski, J. Alloys Compd. 509 (2011) S197–S201.
[20] R. Li, S. Kumar, S. Ram, M. Stoica, S. Roth, J. Eckert, J. Phys. D: Appl. Phys. 42 (2009) 085006.
[21] H. Kronmüller, J. Appl. Phys. 52 (3) (1981) 1859–1864.
[22] N. Moser, H. Kronmüller, W. Frank, J. de Phys. 42 (1981) 647–665.
[23] M. Nabiałek, M. Dośpiał, M. Szota, P. Pietrusiewicz, Mater. Sci. Forum 654–656 (2010) 1074–1077.
[24] M. Vazqeuez, W. Fernengel, H. Kronmüller, Phys. Status Solidi A 115 (1989) 547–553.
[25] T. Holstein, H. Primakoff, Phys. Rev. 59 (1941) 388–394.
[26] O. Kohmoto, J. Appl. Phys. 53 (11) (1982) 7486–7490.